Supplementary Information

Photovoltaic-driven stable electrosynthesis of H_2O_2 in simulated seawater and its disinfection application

Yichan Wen [†], Youyou Feng[‡], Jing Wei [‡*], Ting Zhang[†], Chengcheng Cai[†], Jiyi Sun[†], Xufang Qian[† *], Yixin Zhao[†*]

[†] *School of Environmental Science and Engineering, Frontiers Science Center for Transformative Molecules, Shanghai Jiao Tong University, Shanghai 200240, P. R. China.*

[‡] *Institute of Analytical Chemistry and Instrument for Life Science, The Key Laboratory of Biomedical Information Engineering of Ministry of Education, School of Life Science and Technology, Xi'an Jiaotong University, Xi'an, 710049, P. R. China*

*Corresponding Authors.

E-mail: qianxufang@sjtu.edu.cn (Xufang Qian); yixin.zhao@sjtu.edu.cn (Yixin Zhao)

EXPERIMENTAL

Preparation of N-doped carbon catalysts: Melamine resin was synthesized with the existence of a crosslinking agent triblock copolymer F127. In a typical procedure, 6.3 mL of formaldehyde solution (37%) was added into a 100 mL round bottom flask. And then 3.9 g of melamine and 0.13 g of F127 were added. The mixture was refluxed and thoroughly polymerized at 80 °C until the solution was transparent. The obtained mixture was subsequently washed with 100 mL of an alkaline ethanol solution, water and ethanol until the pH was 7, then the solvents were removed by heating evaporation to obtain melamine resin. The melamine resin was subjected to pyrolyze 3h at the temperatures of 400 °C, 500 °C, 600 °C, 700 °C with a heating rate of 2 °C min^{-1}. The obtained grey/black powder were designated as NC400, NC500, NC600 and NC700, respectively. The catalyst powders were ball milled to fine particle to enhance their dispersibility in the following slurries preparation.

Material characterization: The morphologies of N-doped carbon catalysts were carried out by Hitachi S-4800 scanning electron microscopy (SEM) and Talos F2000X G2 transmission electron microscopy (TEM). The XPS was characterized by a Kratos Axis Ultra DLD type energy dispersive spectroscope, the testing conditions were as follow: Al-K α, the emitter served as the excitation light source with a resolution of 0.48 eV.

Electrochemical measurements: The RRDE were conducted using the ALS-3A instrument, and a d = 5.0 mm glassy carbon disk with a platinum ring electrode was utilized as the electrode substrate. The catalysts were dispersed in a 0.5wt% Nafion® binder solution to obtain a uniform and stable catalyst slurry (10 mg mL^{-1}). The catalyst ink was dropped onto the RRDE, and dried at room temperature, the final optimum catalyst loading per unit area was 0.5 mg cm^{-2}. Firstly, O_2 was blown in the electrolyte for 30 minutes to maintain O_2 saturation. The specific measurement parameters were as follows: the scanning speed of 10 mV s^{-1}, the ring collection voltage (E_{ring}) of 1.2 V_{RHE}, electrode rotating of 900 rpm, 1600 rpm, 2500 rpm and 3600 rpm were selected. A electron collection efficiency (N) of 40.0% was determined by the redox reaction of $[Fe(CN)_6]^{4-}$/$[Fe(CN)_6]^{3-}$. The H_2O_2 selectivity was calculated by the equation (1), in where I_D represented the current density of the rotating disk electrode, I_R represented the current density of the ring:

$$H_2O_2\% = 200 \times \frac{I_R/N}{I_D + I_R/N} \quad (1)$$

The *n* of the ORR process was calculated by the equation (2):

$$n = 4 \times \frac{I_D}{I_D + I_R/N} \quad (2)$$

Electrochemical properties were investigated using a CHI electrochemical station (CHI 660E) in a standard three-electrode H-type cell. A proton exchange membrane (PEM) of Nafion® 211E was used to separate the cathode and anode, a saturated calomel electrode (Hg/HgO) was used as the reference electrode and a platinum mesh was used as the counter electrode. A gas diffusion electrode with geometric area of 1cm^2 and catalyst loading of 0.5 mg cm^{-2} was used as the working electrode, NaCl solution (35mL 0.5M) was added to each electrolyte chamber in the H-cell. Before the typical electrolysis of H_2O_2, the electrode was activated and stabilized by scanning from 0.5 V_{RHE} to -0.5 V_{RHE} at 1 mV s^{-1} for 20 cycles.

Photovoltaic-driven H_2O_2 electrosynthesis: An electrochemical flow-type reactor was used to evaluate the industrial-relevant performance of NC600, which included two stainless steel serpentine flow field plates and one electrolyte chamber of PTFE with 1.6 cm ◊ 1.6 cm geometric cavity. A gas diffusion electrode with geometric area of 2.56 cm^2 and catalyst loading of 0.5 mg cm^{-2} was used as the cathode, an iridium plated titanium mesh was used as the anode and a Nafion® 211E was used as the PEM. Both anode and cathode were circulated or flowed by the electrolyte of 500 mL of 0.5M NaCl. The flow rates of O_2 and anodic, cathodic electrolytes were 100 mL/min, 50 mL/min and 1 mL/min, respectively. A photovoltaic device (40W, 570mm×410mm×25mm) was used as the power supply, and a lithium-ion battery with an output voltage of 5V was used as the energy storage module. A xenon light with the sunlight intensity was used to simulate stable sunlight conditions. The instantaneous data of current and voltage were displayed and recorded by a source meter (Keithley 2400).

The H_2O_2 concentrations of electrolyte fluids (10 mL) flowing out of flow cell were detected by potassium permanganate titration process by the equation (3):

$$2MnO_4^- + 5H_2O_2 + 6H^+ \rightarrow 2Mn^{2+} + 5O_2 + 8H_2O \quad (3)$$

The H_2O_2 yield was calculated by the equation (4):

$$H_2O_2 \text{ production rate 1} = \frac{\text{Generated } H_2O_2\ (mmol)}{\text{Weight of catalyst (mg)} \times \text{ Number of hours (h)}} \quad (4)$$

The H_2O_2 selectivity was calculated by the equation (5):

$$FE = \frac{\text{Generated } H_2O_2\ (mmol)}{\text{Theoratical generated } H_2O_2\ (mmol)} \times 100\% \quad (5)$$

Disinfection measurements: The monoclonal of *E. coli* and *S. aureus* on the solid Luria Bertani (LB) agar plate was transferred to 20 mL of liquid LB medium and cultured at 37 °C for 12 h under 200 rpm rotation. Then the bacteria were diluted to 10^8 CFU mL^{-1} with PBS. The as-prepared bacteria solution (500 μL) was mixed with H_2O_2 (0.3 M) and NaCl (0.5 M) solution for 10 min. Then, the solution was placed on the solid medium by spread plate method and cultured for 24 h. The bacteria colonies were counted. Control experiments were performed in parallel without H_2O_2 or NaCl. SYTO-9 (30 μL, 0.2 mM) and propidium iodide (PI, 30 μL, 0.2 mM) were used to stain the live and dead bacteria. The triplicates of each sample were repeated. The SEM images of bacteria were taken after the gradient dewatering procedure. The injury model was built to evaluate the antibacterial effect of H_2O_2 solution *in vivo*. The Kunming mice were purchased from the Experimental Animal Center of Xi'an Jiaotong University. Four groups of 12 male Kunming mice (6-8 weeks, 18-22 g, and three mice per group) with a *ca*. 20 mm^2 wound were used. *E. coli* cells (50 μL, 3×10^7 CFU mL^{-1}) were injected to the wound area to build the infected wound model. The mice were divided into three groups: blank, 0.5M NaCl, and 1wt% H_2O_2 + 0.5M NaCl groups. The volume of the solution was 50 μL. The weights of mice and photographs of wounds were recorded every day, and the corresponding wound areas were calculated. The wound situation was stained by hematoxylin and eosin (H&E). To demonstrate the biosafety of the material, the blood samples of both the healthy group and the H_2O_2 treated group were collected after 9 days to perform blood biochemical detection. The main organs of both groups were collected for H&E stain. All animal procedures were in accord with the guidelines of the Institutional Animal Care and Use Committee.

RESULTS

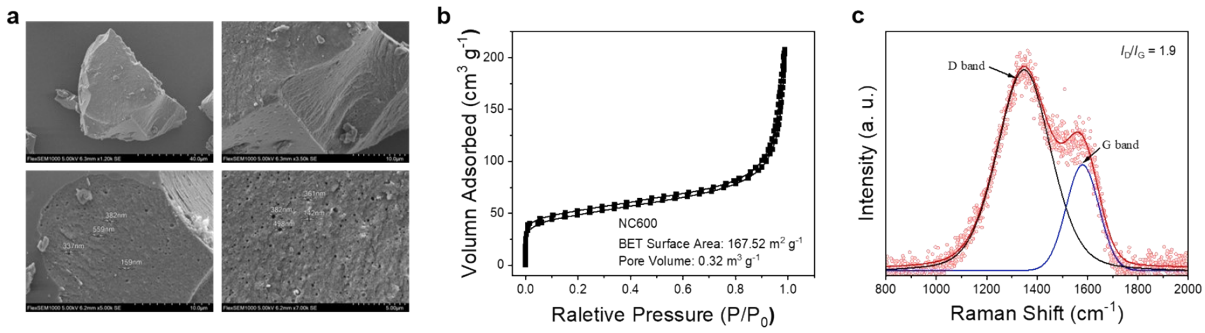

Figure S1. The morphology and pore structure of NC600 catalyst. a) Scanning electron microscopy (SEM) image; b) N_2 adsorption–desorption isotherm; c) Raman spectra.

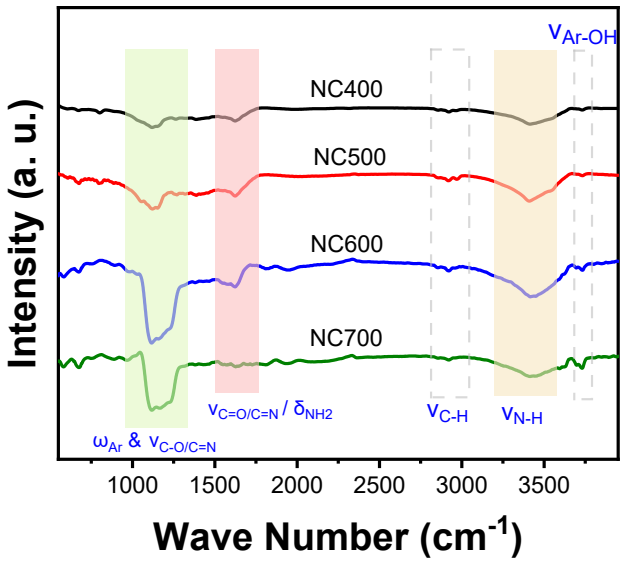

Figure S2. The FTIR spectra of N-doped carbon catalysts.

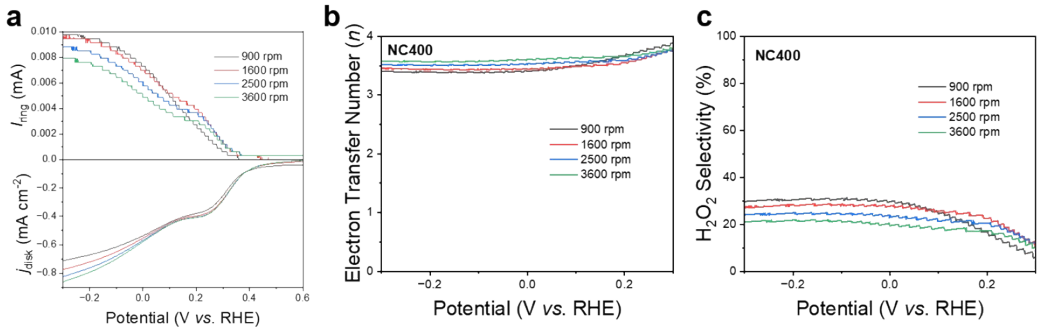

Figure S3. The RRDE characterization of NC400 catalyst. a) LSV curve with the ring electrode collected at a constant potential of 1.23 V_{RHE}; b) *n* of NC400; b) H_2O_2 selectivity of NC400.

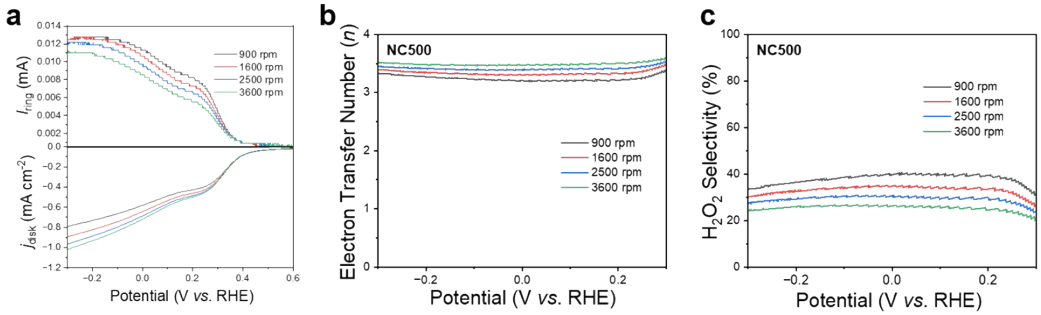

Figure S4. The RRDE characterization of NC500 catalyst. a) LSV curve with the ring electrode collected at a constant potential of 1.23 V_{RHE}; b) *n* of NC500; b) H_2O_2 selectivity of NC500.

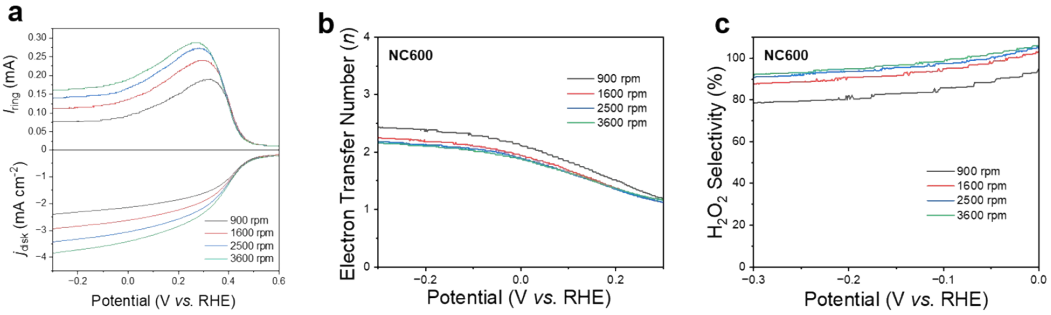

Figure S5. The RRDE characterization of NC600 catalyst. a) LSV curve with the ring electrode collected at a constant potential of 1.23 V_{RHE}; b) *n* of NC600; b) H_2O_2 selectivity of NC600.

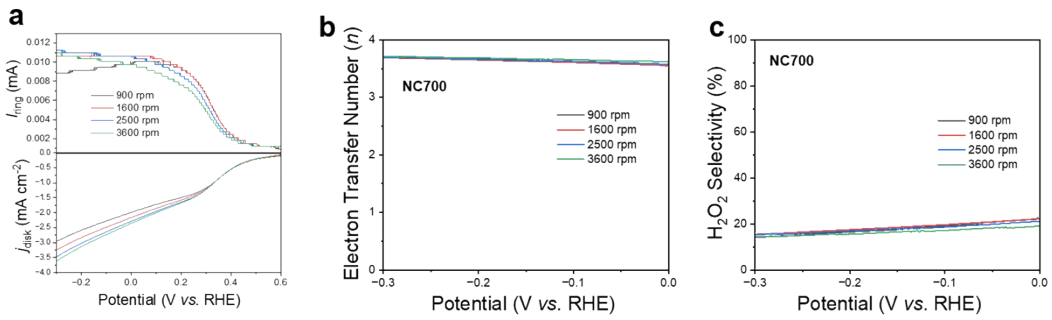

Figure S6. The RRDE characterization of NC700 catalyst. a) LSV curve with the ring electrode collected at a constant potential of 1.23 V_{RHE}; b) *n* of NC700; b) H_2O_2 selectivity of NC700.

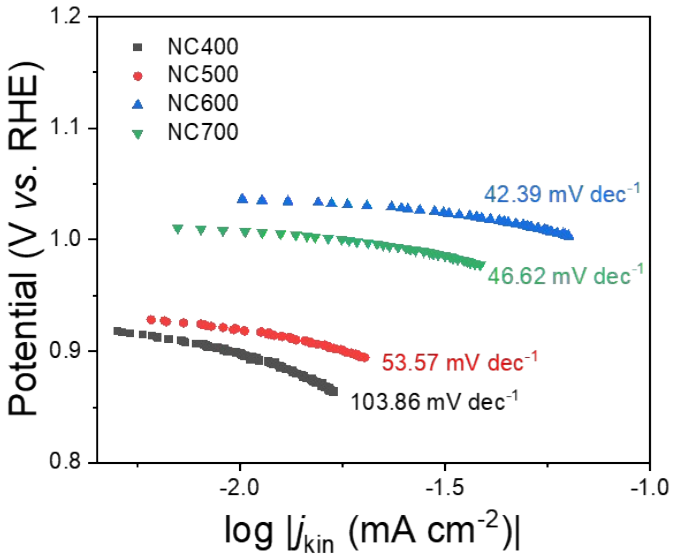

Figure S7. The Tafel slope curves of N-doped carbon catalysts.

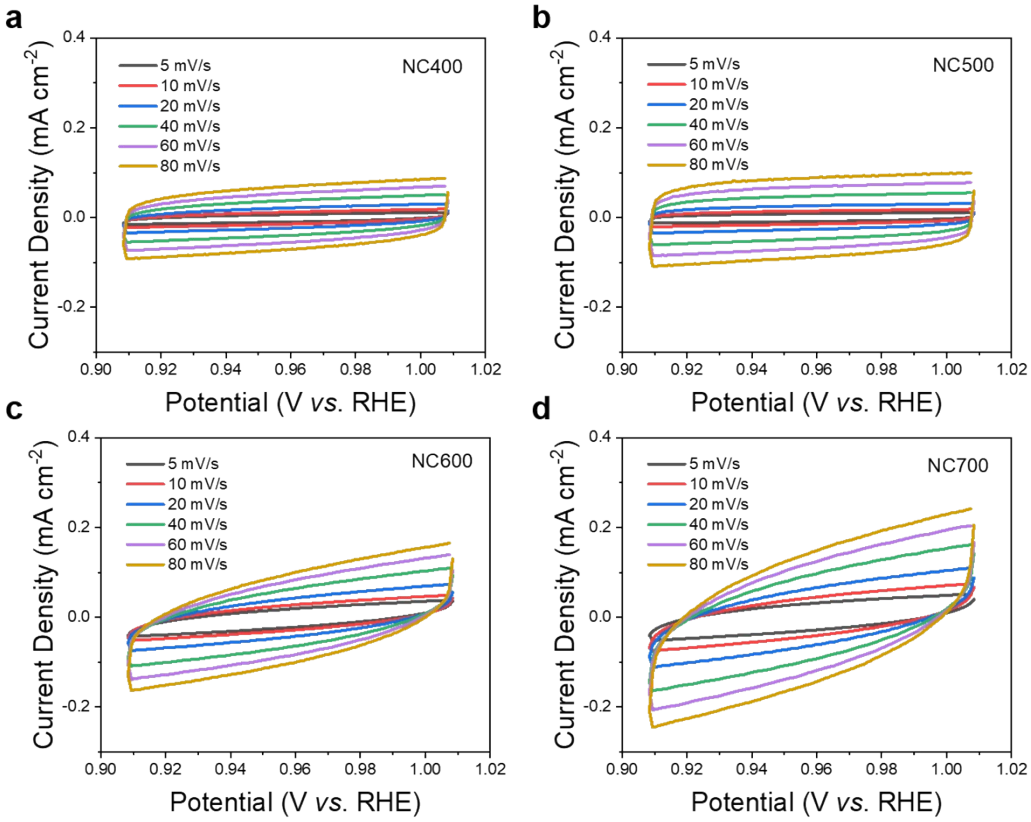

Figure S8. ESCA characterization of N-doped carbon catalysts. a) NC400; b) NC500; c) NC600; d) NC700.

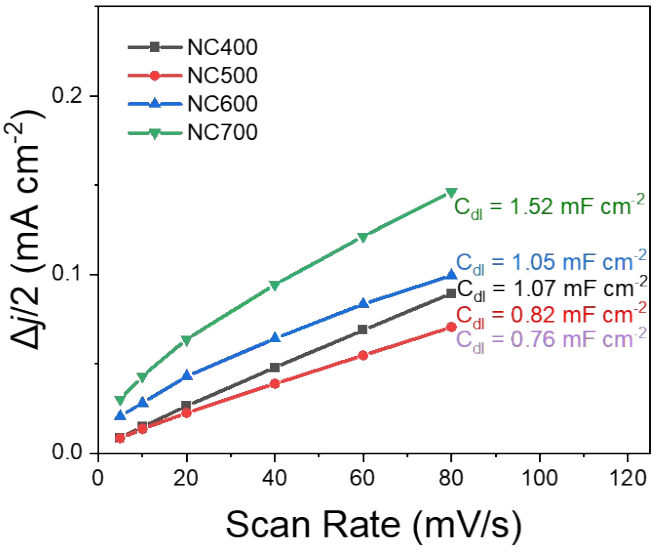

Figure S9. Double layer capacitance (C_{dl}) of N-doped carbon catalysts.

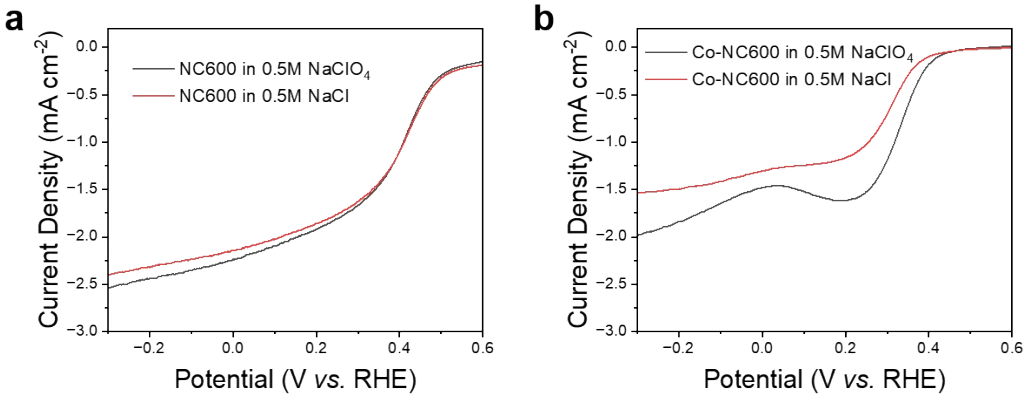

Figure S10. LSV curves of (a) NC600 and (b) Co-NC600 in 0.5M $NaClO_4$ and 0.5M NaCl characterized by RDE. The synthesis of Co-NC600 is the same as NC600, except for adding 0.03 mol of cobalt nitrate hexahydrate.

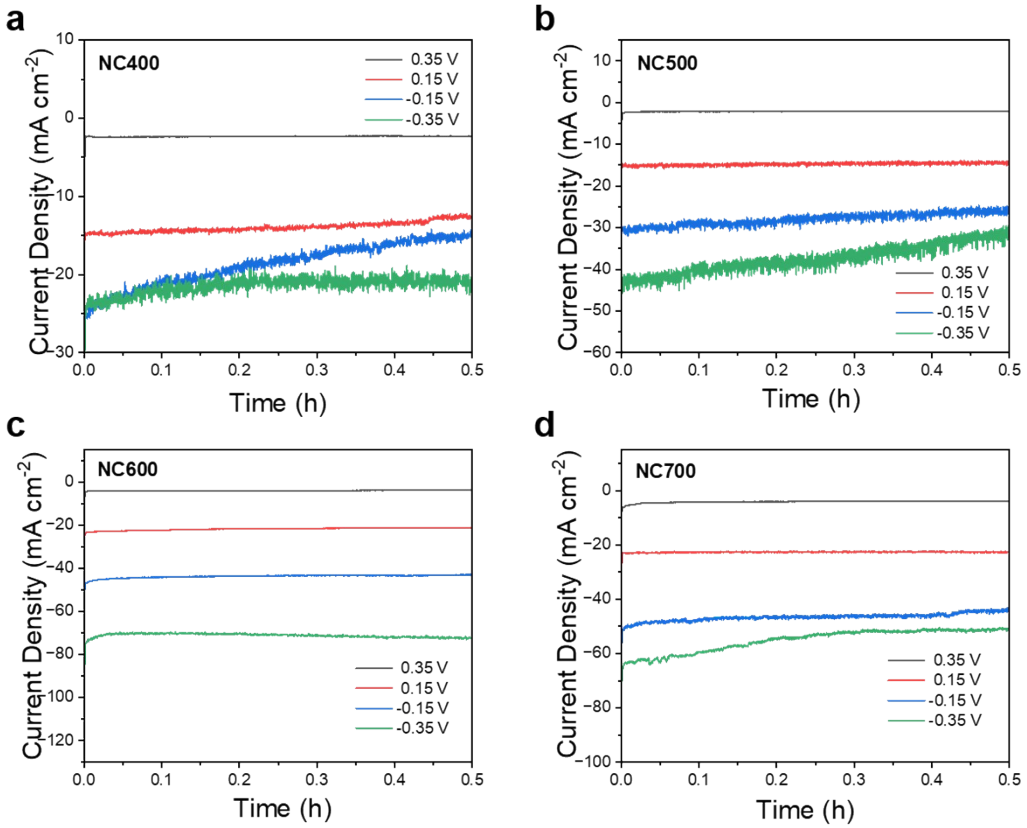

Figure S11. The curves of current density over time under different electrolysis voltages of N-doped carbon catalysts. a) NC400; b) NC500; c) NC600; d) NC700.

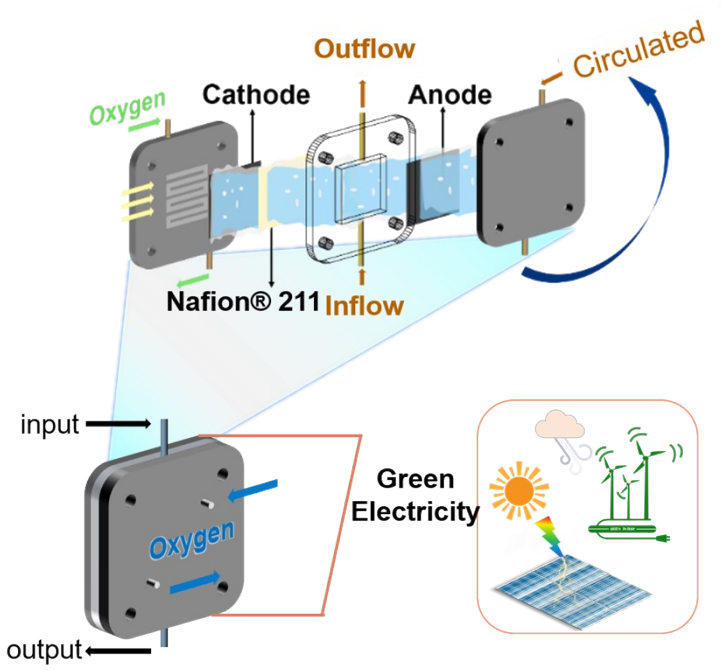

Figure S12. The device scheme of the two-electrode system.

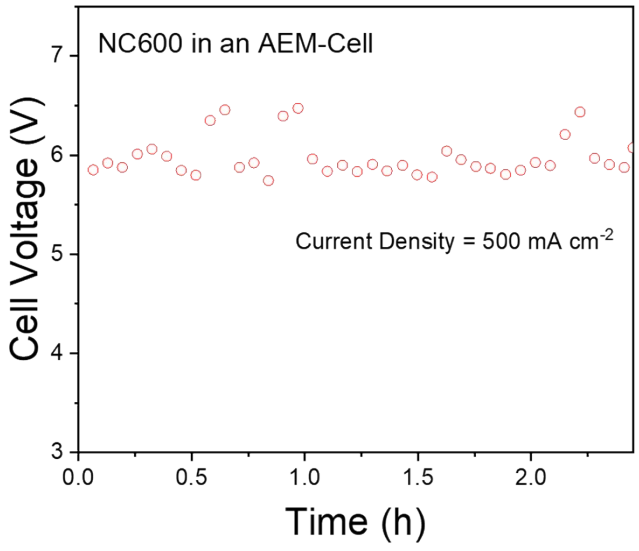

Figure S13. The curve that cell voltage varied with reaction time at the current density of 500 mA cm^{-2}, in which the NC600 was configurated in a two-electrode flow cell with an anion exchange membrane (AEM).

Figure S14. The digital photos of the photovoltaic driven H_2O_2 electrosynthesis.

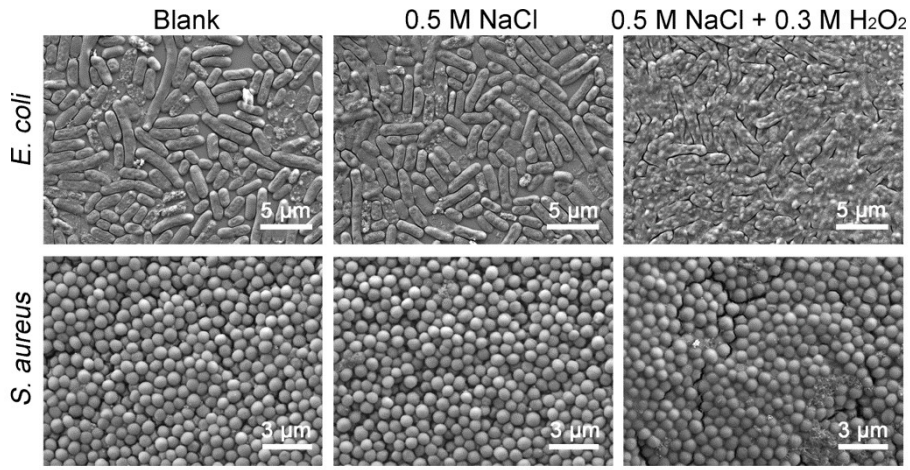

Figure S15. The SEM images of flat coated E. coli and S. aureus treated with blank, 0.5M NaCl and the obtained 0.3M H_2O_2 + 0.5M NaCl solution.

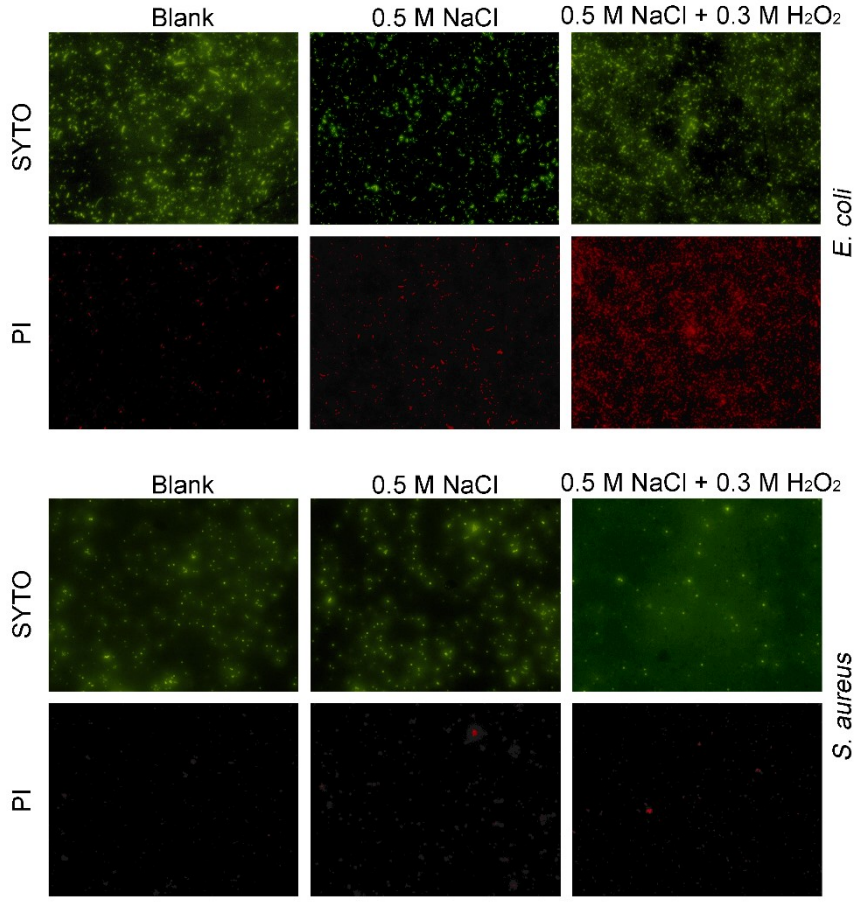

Figure S16. The images under the fluorescence microscope of flat coated E. coli and S. aureus treated with blank, 0.5M NaCl and the obtained 0.3M H_2O_2 + 0.5M NaCl solution.

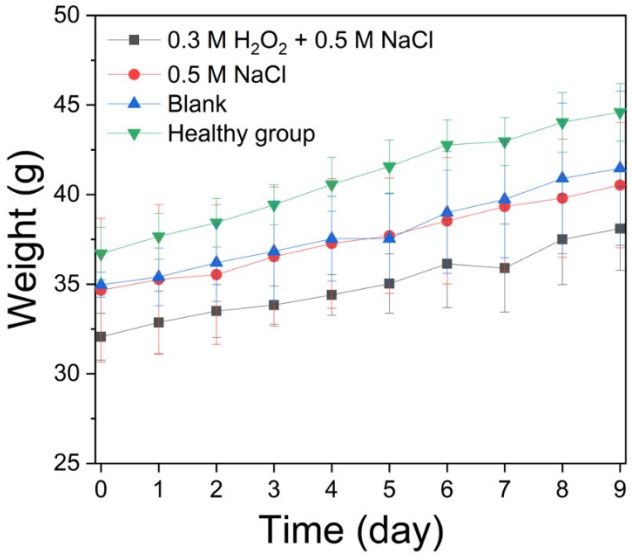

Figure S17. Weight changes of mice treated with healthy group, blank, 0.5M NaCl and the obtained 0.3M H_2O_2 + 0.5M NaCl solution.

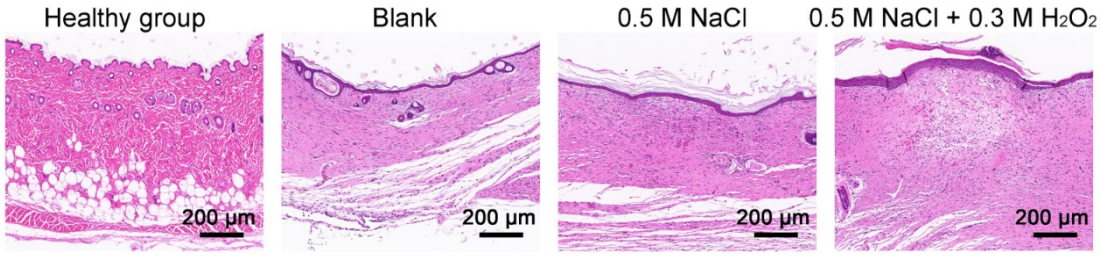

Figure S18. H&E staining results of mice wounds treated with healthy group, blank, 0.5M NaCl and the obtained 0.3M H_2O_2 + 0.5M NaCl solution.

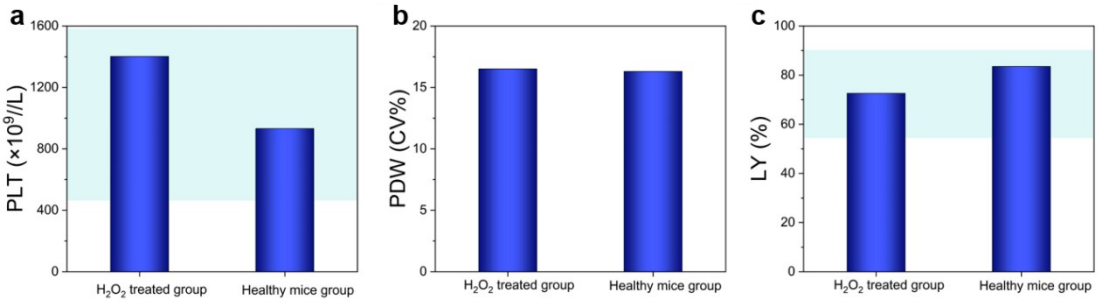

Figure S19. Hematology analysis of mice treated with obtained H_2O_2 solution and healthy group. (a) PLT, (b) PD, (c) LY. Results are presented as mean ± S.D. (n = 3)

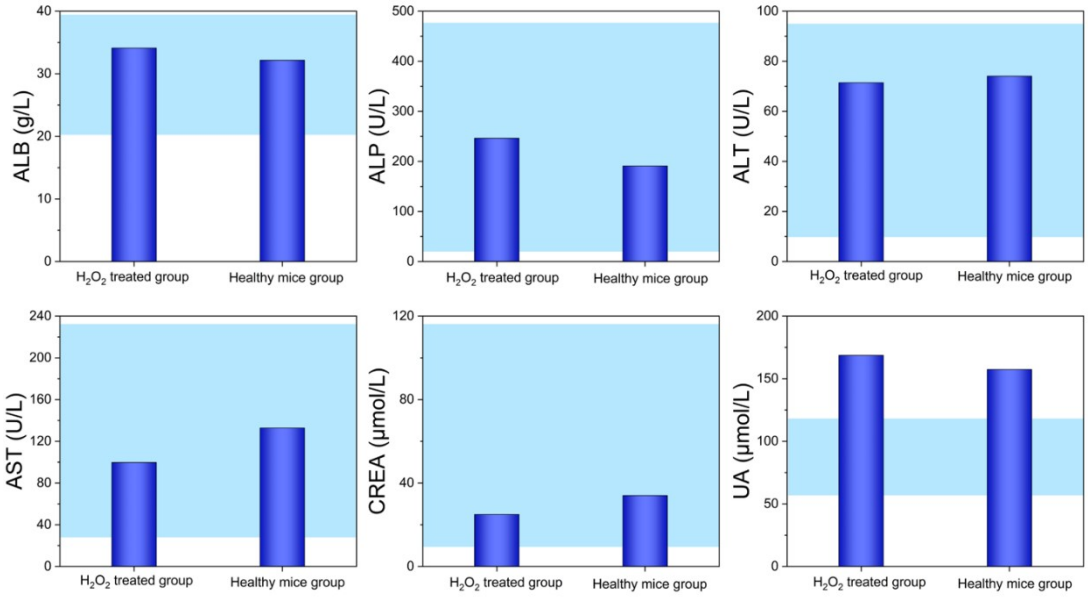

Figure S20. Hematology analysis of the mice treated with obtained H_2O_2 solution and healthy group. (a) ALB, (b) ALP, (c) ALT, (d) AST, (e) CREA, (f) UA.

Supplementary Note. Technoeconomic & energy analysis

The technoeconomic and energy analysis are calculated to identify the feasibility of green power driven H_2O_2 electroproduction.[1, 2]

The assumptions are listed as follows:

1. The H_2O_2 production capacity of the plant is 1 tonne per day with the purity of 70 %.
2. The cost of catalysts and membrane is 2800 \$/m^2.
3. The flow cell cost is assumed 10000 \$/m^2 with a lifespan of 30 years.
4. The price of green power is 0.035 \$/kWh.
5. The cost and energy analysis of the separation is calculated based on the vacuum distillation technology.[3, 4]
6. The capacity factor is assumed to be 0.9.
7. The maintenance cost is assumed to be 10 % of the capital cost.
8. The balance cost of plant is assumed to be 50 % of the capital cost.
9. The installation cost is assumed to be 10 % of the capital cost.
10. The operational cost is assumed to be 10 % of the electricity cost.
11. The O_2 price is 40 \$/Mt and 75 % of the O_2 is recovered from the anode side.

The cost components and their formula are as follows:

$$Total\ surface\ area\ (m^2) = \frac{Total\ current\ (A)}{Current\ density\ (A/m^2)}$$

$$Total\ current\ (A) = \frac{Plant\ capacity\ (ton/day)\ \times n\ \times F\ constant\ (C/mol)}{H_2O_2\ molar\ mass\ (g/mol)\ \times 24\ (day/h)\ \times 3600\ (s/h)\ \times FE\ (\%)}$$

$$Flow\ cell\ cost\ (\$/ton)\ = \frac{Total\ surface\ area\ (m^2) \times Flow\ cell\ cost\ (\$/m^2)}{Capacity\ factor\ \times Cell\ lifespan\ (day) \times H_2O_2\ production\ (ton/day)}$$

$$Electricity\ consumption\ (kWh/ton) = \frac{Totalcurrent\ (A)\ \times Cell\ voltage\ (V) \times 24\ (h/day)}{Plant\ capacity\ \times 1000\ (W/kW)}$$

$$Electricity\ cost\ (\$/ton) = Electricity\ consumption\ (kWh/ton) \times Electricity\ cost\ (\$/kWh)$$

Table S1. Comparison of this work and recently reported carbon-based catalysts for H_2O_2 production via ORR in neutral electrolytes.

Catalyst	J_{total} (mA cm^{-2})	Stability (h)	H_2O_2 Production (mmol g_{cat}^{-1} h^{-1})	Electrolyte
NC600(this work)	**500**	**200**	**34.7**	**0.5M NaCl***
CoPc-CNT(O)[1]	300	100	26.1	1M Na_2SO_4*
CBNO[5]	100	24	13.4	0.1M Na_2SO_4*
N,O-$CNS_{0.5}$[6]	~100	24	6.7	0.1M K_2SO_4*
Co-N-C[7]	50	24	4.5	0.5M NaCl*
h-SnO_2[8]	120 mA	20	3.9	0.1M Na_2SO_4*
CB-10%[9]	200	100	3.7	SE[a] *
AC-MW5.0/CPF[10]	~12	0.5	1.9	0.1M K_2SO_4#
N-C_{800}[11]	~50	10	0.6	0.5M NaCl#

* Represent the catalyst was fabricated in a flow cell.

Represent the catalyst was fabricated in a H-cell.

[a]SE: solid electrolyte with neutral DI water flow.

Reference

[1] B.-H. Lee, H. Shin, A.S. Rasouli, H. Choubisa, P. Ou, R. Dorakhan, I. Grigioni, G. Lee, E. Shirzadi, R.K. Miao, J. Wicks, S. Park, H.S. Lee, J. Zhang, Y. Chen, Z. Chen, D. Sinton, T. Hyeon, Y.-E. Sung, E.H. Sargent, Supramolecular tuning of supported metal phthalocyanine catalysts for hydrogen peroxide electrosynthesis, Nature Catalysis, 6 (2023) 234-243.

[2] W.R. Leow, Y. Lum, A. Ozden, Y.H. Wang, D.H. Nam, B. Chen, J. Wicks, T.T. Zhuang, F.W. Li, D. Sinton, E.H. Sargent, Chloride-mediated selective electrosynthesis of ethylene and propylene oxides at high current density, Science, 368 (2020) 1228-1233.

[3] T. Darczuk, M. Kania, P. Romanowski, B. Rudnik, I. Satkowski, Method for concentrating and purifying aqueous hydrogen peroxide solutions, involves concentrating hydrogen peroxide, feeding solution into column, evaporating, and adding mixture of nitric acid and stabilizer with demineralized water, Grupa azoty zaklady azotowe pulawy sa (azot-non-standard) grupa azoty zaklady azotowe pulawy sa (azot-non-standard).

[4] M. Mishra, A. Feidler, Ullmann's encyclopedia of industrial chemistry, fifth edition on CD-ROM, Journal of the American Chemical Society, 120 (1998) 6197-6198.

[5] Z. Song, X. Chi, S. Dong, B. Meng, X. Yu, X. Liu, Y. Zhou, J. Wang, Carboxylated Hexagonal Boron Nitride/Graphene Configuration for Electrosynthesis of High-Concentration Neutral Hydrogen Peroxide, Angewandte Chemie-International Edition, 63 (2024)

e202317267.
[6] L. Jing, Q. Tian, W. Wang, X. Li, Q. Hu, H. Yang, C. He, Unveiling Favorable Microenvironment on Porous Doped Carbon Nanosheets for Superior H_2O_2 Electrosynthesis in Neutral Media, Advanced Energy Materials, 14 (2024) 2304418.
[7] Q.L. Zhao, Y. Wang, W.H. Lai, F. Xiao, Y.X. Lyu, C.Z. Liao, M.H. Shao, Approaching a high-rate and sustainable production of hydrogen peroxide: oxygen reduction on Co-N-C single-atom electrocatalysts in simulated seawater, Energy & Environmental Science, 14 (2021) 5444-5456.
[8] Y. Zhang, M. Wang, W. Zhu, M. Fang, M. Ma, F. Liao, H. Yang, T. Cheng, C.-W. Pao, Y.-C. Chang, Z. Hu, Q. Shao, M. Shao, Z. Kang, Metastable Hexagonal Phase SnO_2 Nanoribbons with Active Edge Sites for Efficient Hydrogen Peroxide Electrosynthesis in Neutral Media, Angewandte Chemie-International Edition, 62 (2023) e202218924.
[9] C. Xia, Y. Xia, P. Zhu, L. Fan, H. Wang, Direct electrosynthesis of pure aqueous H_2O_2 solutions up to 20% by weight using a solid electrolyte, Science, 366 (2019) 226-231.
[10] M. Wang, Y. Li, J. Xu, L. Guan, Surface oxidation of commercial activated carbon with enriching carboxyl groups for high-yield electrocatalytic H_2O_2 production, Nanotechnology, 35 (2024) 025706.
[11] N. Wang, S.B. Ma, R.Y. Zhang, L.F. Wang, Y.A. Wang, L.H. Yang, J.H. Li, F. Guan, J.Z. Duan, B.R. Hou, Regulating N Species in N-Doped Carbon Electro-Catalysts for High-Efficiency Synthesis of Hydrogen Peroxide in Simulated Seawater, Advanced Science, 10 (2023) 2302446.